



ARTICLE

Forest Fire Assessment and Analysis in Liangshan, Sichuan Province Based on Remote Sensing

Yiwei Hua¹ and Xingdong Wang^{1,*}¹ College of Information Science and Engineering, Henan University of Technology, Zhengzhou 450001, China

Abstract

Because of the special geographical location, dry weather, high temperature and dense vegetation in Liangshan, Sichuan, it is easy to cause forest fires, so it is of great significance to use remote sensing data to evaluate forest fires in Liangshan, Sichuan. In this paper, the forest fire in Muli County, Liangshan, Sichuan Province on March 28th, 2020 was evaluated by using Landsat-8 remote sensing data which can be obtained free of charge. The NDVI of the pre-processed remote sensing images before and after the fire was calculated respectively. After the difference was made, the threshold of the classification of fire and non-fire areas was determined according to the maximum inter-class difference threshold method, and then the over-fire areas were extracted, and the interference was eliminated by open operation. And using the DEM data of the study area, combined with the topography of the study area, the over-fire area is analyzed. The results show that the "3.28" forest fire in Muli County, Sichuan Province, which is studied, belongs to a serious forest fire according to the burned area.

Keywords: forest fire, remote sensing assessment, NDVI

Academic Editor:

Jinchao Chen

Submitted: 09 June 2023**Accepted:** 11 October 2023**Published:** 17 October 2023**Vol. 1, No. 1, 2023.**

registering DOI

***Correspondence Author:**

✉ Xingdong Wang

xdwang8888@163.com

Citation

Y. Hua & X. Wang (2023). Forest Fire Assessment and Analysis in Liangshan, Sichuan Province Based on Remote Sensing. *IECE Transactions on Internet of Things*, 1(1), 15–21.

© 2024 IECE (Institute of Emerging and Computer Engineers Inc). Personal use is permitted, but republication/redistribution requires IECE permission.

1 Introduction

In recent years, due to some extreme weather events and improper use of fires, forest fires have occurred from time to time worldwide. Forest fires are a kind of natural disasters with great destructiveness, high risk and difficult to carry out rescue work. Due to the large forest area, complex terrain and rugged roads in China, it is difficult to fully monitor the fire situation in the forest by using the traditional monitoring method [1]. In this case, it is inevitable to use remote sensing satellites to monitor forest fires macroscopically and evaluate them. Remote sensing can conduct real-time observation on a large area of research area, grasp the fire situation in time, and minimize the huge losses caused by fire [2]. Liangshan in Sichuan has less precipitation and special geography in winter and spring, which makes the frequency of forest fires in this region higher than other regions in China. Therefore, it is of great practical significance to evaluate forest fires in Liangshan based on remote sensing data.

Compared with the traditional field investigation, the multispectral and hyperspectral sensors of remote sensing satellites can realize the large-scale synchronous identification of high temperature and flame, and quickly judge the damage caused by them, which has more advantages in forest fire assessment [3–5]. Long et al. developed a global 30 m spatial resolution remote sensing product based on the Google

Earth Engine, and shared it publicly, and Liu et al. used the normalized difference combustion index (dNBR) to assess the damage level of forest fires that occurred on 2 May 2017 in Birahe Forest Farm, Inner Mongolia [6]. Using remote sensing satellites to collect vegetation information has the characteristics of large scale, high precision and low cost. It is an important aspect of remote sensing technology to extract information about forest fires from remote sensing images according to the intensity relationship between remote sensing images and on-the-spot investigation of forest fires [7, 8].

2 Data and Methods

2.1 Overview of the Study Area

In March 2020, Muli County is in the season of high temperature and less rainfall in spring (Topographic map is shown in Fig. 1). If it encounters dry thunder weather, it may cause fire in a short time [9]. The fire area belongs to the mountainous area of Liangshan Prefecture, with relatively high altitude, single tree species and more oil. After the forest fire in this area, the hot air rises, which affects the direction of the wind. In addition, the complex terrain makes the wind direction easy to change, making the fire duration longer and unpredictable [10]. The forest fire in Xiangjiao Town, Muli County, Liangshan Prefecture on March 28, 2020 was studied in this paper.

On March 30, the fire was first distributed in the triangle area formed by Youyouping Village, Dujia Village and Xiangjiao Village, and the fire was large and had a trend of spreading. On 31st, the fire area expanded rapidly, and the fire in the directions of Shangyaopu and Dapo townships was large, showing a trend of spreading to Baidiao township. On April 1, the fire moved northeast. The main fire areas were Shangyaopu, Gamiping and Dapoxiang. There were a large number of white smoke in the fire area, falling with the wind in the northeast area of the fire. The fire was controlled on April 4 [11].

2.2 Data Acquisition and Preprocessing

The data used in this paper are from the geospatial data cloud, downloaded are landsat-8 OLI_TIRS satellite digital products and SRTMDem 90 M resolution original elevation data products [12]. In order to better determine the study area, the downloaded Landsat-8 data were preprocessed by atmospheric correction, radiation correction and clipping to obtain the study area.

2.3 Extraction Method of Fire Area

In remote sensing images, there is a great difference in the reflectance of overfire pixels and non-overfire pixels in thermal infrared and other bands. According to this feature, the hidden characteristics in remote sensing images can be better excavated. Moreover, combined with some physical characteristics changes before and after the fire in traditional methods [13], the extraction accuracy of overfire areas can be further improved. NDVI is used to extract the fire traces. The calculation formula is as follows:

$$NDVI = \frac{NIR - Red}{NIR + Red} \quad (1)$$

Which, NIR and Red correspond to the gray values of the fifth band (near infrared) and the fourth band (red) in Landsat 8 data respectively [14]. The vegetation coverage of the affected area before and after the fire is quite different, so the difference between the two images processed by NDVI (before the fire minus after the fire) is large. At any point in the fire area, the NDVI value before the fire is large, and the NDVI value after the fire decreases. Therefore, the larger positive area after the difference is the overfire area, as shown in Fig. 1.

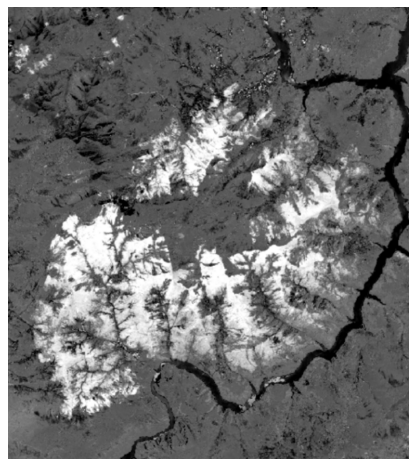


Figure 1. Images after NDVI.

2.4 Image Binaryzation

The remote sensing image after NDVI difference is gray image. Although the approximate fire area can be seen, there is no way to obtain the specific overfire area. Therefore, the two gray images should be binarized to further separate the fire area.

The image binarization processing to select the appropriate threshold, the current commonly used threshold segmentation methods are histogram threshold method, iterative threshold method, Otsu

algorithm. The error of histogram threshold is large, and the noise of iterative threshold method is large [15]. So the Otsu algorithm is used to determine the threshold. The Otsu algorithm uses the gray level of the image to cluster and get [16]. Firstly, the normalized image is transformed into the gray image of 0 ~ 255. Assuming that any point on the normalized image is x , the equation (2) is transformed into the gray image of 0 ~ 255.

$$x_{\text{scale}} = \frac{x - x_{\text{min}}}{x_{\text{max}} - x_{\text{min}}} * 255 \quad (2)$$

Which, x_{scale} is the converted gray value, x_{min} is the minimum value in the normalized image, and x_{max} is the maximum value. Then, each gray value in the image gray level 0 – 255 is traversed, and the inter-class variance when each gray value is used as the threshold is calculated. Finally, the gray value corresponding to the minimum inter-class variance is the optimal threshold. The threshold of NDVI difference image obtained by Otsu algorithm is 146, and the binary image is shown in Fig. 2.



Figure 2. Binarization image.

2.5 Image Processing Based on Morphology

The binary image can be seen that there are too many debris polygons, that is, the error generated, directly to calculate the fire area, will make the calculation result is too large, so the image morphological open operation processing. The opening operation (equation (3)) is to erode the image first and then expand the image [17].

$$B = A \circ S = (A \otimes S) \oplus S \quad (3)$$

This formula uses structural element S to conduct corrosion operation on A , and then uses structural element S to conduct expansion operation on corrosion

results to obtain the final open operation result B . After the open operation, the area of the combustion area will not be changed when the polygon that does not belong to the combustion area is effectively removed [18, 19]. The binarization image after NDVI difference is shown in Fig. 3.

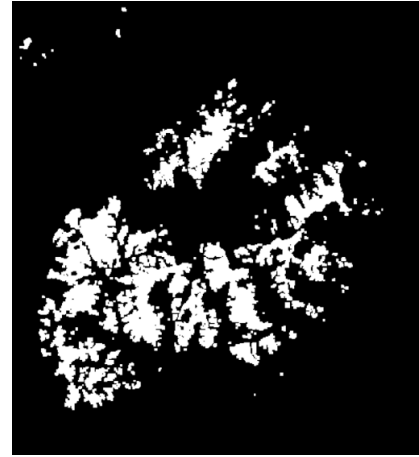


Figure 3. Opened image.

3 Results and Analysis

3.1 Fire Assessment

It can be seen that after opening operation, there are still a small number of polygons independent of the fire area, which obviously do not belong to the fire area. Therefore, the fire area is removed by visual interpretation, and then the fire area is extracted. The number of pixels in the fire area is counted and the fire area is calculated by spatial resolution. The area of burned area extracted based on NDVI is 10224.45 hectares, and the results are shown in Fig. 4.

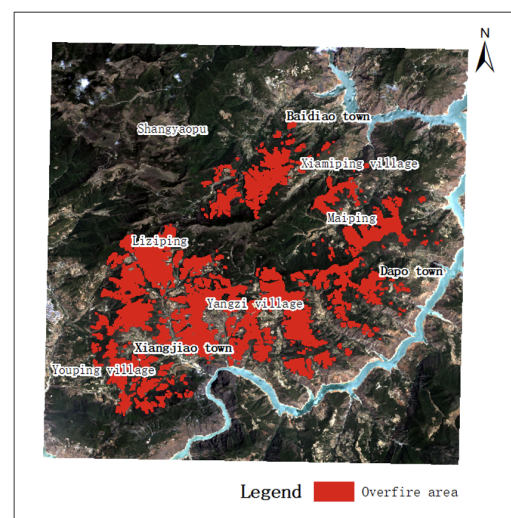


Figure 4. Fire area extracted.

According to the Forest Fire Regulations, forest fires

can be divided into four categories according to the size of the damaged forest area : general forest fires, larger forest fires, major forest fires and particularly major forest fires, and the specific classification criteria are shown in Table 1 [20]. The extracted fire area is greater than 10000 hectares, so the fire is determined to be a particularly significant forest fire.

Table 1. Forest fire classification table.

forest fire class	Classification (affected area)	standard
General forest fires	Less than 1 hectare	
Larger forest fires	1 hectare above but below 100 hectares	
major forest fire	More than 100 hectares but less than 1000 hectares	
Specially significant forest fires	more than 1000 hectares	
forest fire class	Classification (affected area)	standard

3.2 Analysis of Fire Area

With the continuous increase of altitude, the temperature will gradually decrease [21]. Under the standard atmospheric pressure, the temperature will decrease by 6 degrees Celsius with every 1000 m increase of altitude. Moreover, the higher the altitude is, the lower the temperature is, and the greater the relative humidity is. The vegetation has high water content and is not easy to burn. However, the wind speed in high altitude areas is generally large, easy to spread and difficult to rescue. And the steep slope position, water is not easy to store, soil water content decreased, resulting in vegetation coverage reduced, not prone to forest fires. In addition, slope aspect also affects forest fires. The south slope is a sunny slope and receives more solar radiation, so the temperature is high and forest fires are more likely to occur [22].

It can be seen that there are two discontinuous phenomena [23–25] in the extracted fire area [26–28], which is related to the geographical location of the study area and the weather conditions of the day. According to Fig. 5, it can be seen that in the middle of the study area, the terrain is relatively high, and the surrounding terrain is relatively low. In addition, the fire area is not formed one day, and the wind direction has been changing. There is a flash fire, so such a fire area is formed. In order to better analyze the formation of the overfire area, the slope and aspect of the fire area and the study area extracted based on NDVI are

superimposed [29–32], respectively. The slope map of the overfire area is shown in Fig. 6, and the slope map of the overfire area is shown in Fig. 7. Combined with the fire trend figure Fig. 8, the specific analysis is as follows:

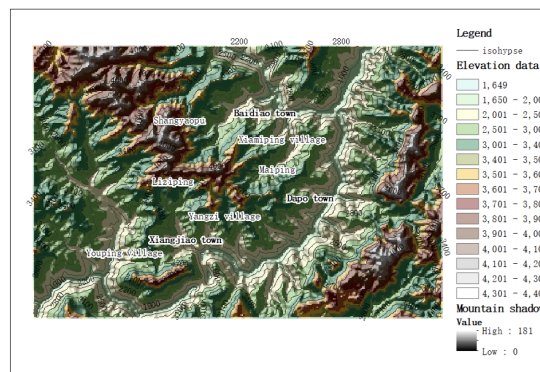


Figure 5. Topographic map of the study area.

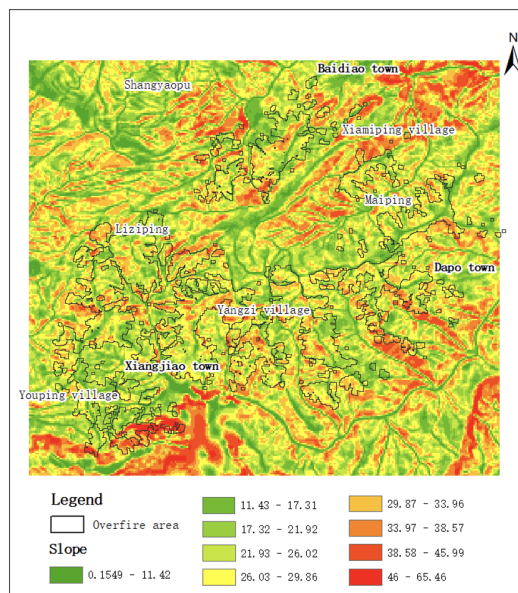


Figure 6. Slope map of fire area.

From March 28 to March 30, the fire area formed a ring in Youyouping Village and Xiangjiao Township. Due to the high elevations in the south of Youyouping Village and the northeast of Liziping Village, reaching about 4000 m, the fire was not easy to spread to it, and the later fire spread to the east. On 31 March, the fire in Liziping was affected by the fire, and a new burning point appeared in the Shangyaopu in the north of Liziping. The wind direction was south on that day, so the fire area spread rapidly to BaiDiao Town. Due to the large slope in the southeast of BaiDiao Town, the vegetation coverage was small, and it was not easy to fire. In addition, the wind direction affected the new ignition point in Gamiping Village, which formed the discontinuity of fire area between BaiDiao Town

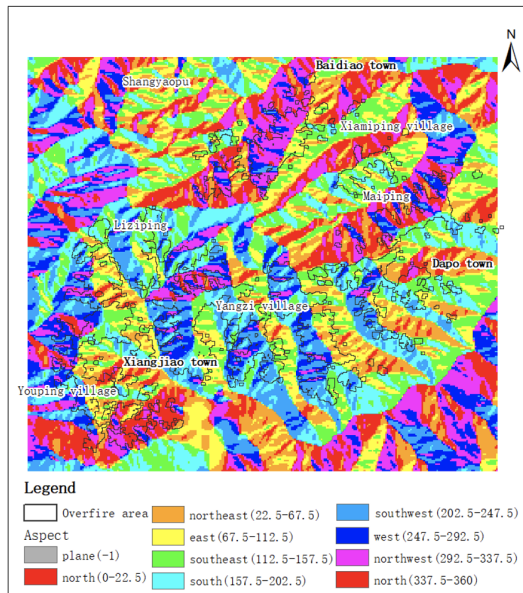


Figure 7. Slope map of fire area.

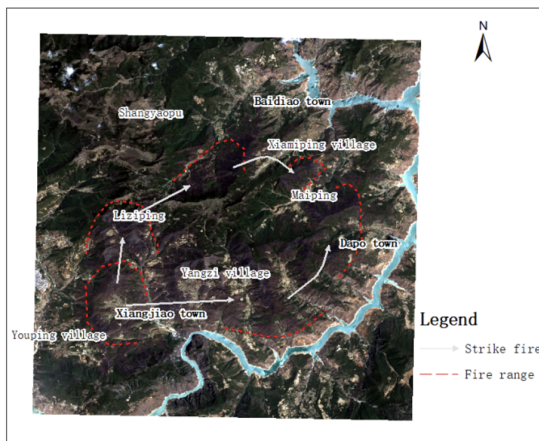


Figure 8. Schematic diagram of fire trend.

and Gamiping Village. Youyoping Village spread northeast to Yangwozi Village and Dapo Village. On April 1, the fire in the southern part of the fire area was effectively controlled, and the fire was gradually smaller. The fire was mainly in Dapo Township and Gamiping Village in the northern part of the fire site. Because the fire in Dapo Township and Gamiping Village was not spread at the same ignition point, the two fire areas were discontinuous.

4 Conclusion

Based on remote sensing data, this paper evaluates the forest fire in Muli County, Liangshan, Sichuan Province on March 28, 2020. The method used is accurate and concludes that:

According to the final calculated area of forest fires, according to the classification of forest fires, the 3.28 forest fires studied in this paper belong to particularly

significant forest fires. Combined with the elevation, slope and aspect of the study area, the formation of forest fire area is analyzed. Considering the influence of various factors on the fire area, it has certain guidance for the prevention of forest fire and post-disaster recovery in the future.

Forest fire assessment based on remote sensing data, in addition to the common study of fire area, can also assess the damage of vegetation, economic losses, etc., for further vegetation restoration in the fire area to develop more appropriate plans. This paper only evaluates some of them, and there is more evaluation content to be further studied.

References

- [1] Zheng, H., Wu, Z., & Wang, W. (2022). Forest fire risk assessment and prevention suggestions in heilongjiang province. *Forestry Science & Technology*, 47(1), 43–46.
- [2] Chen, J., Du, C., Xie, F., & Lin, B. (2016). Allocation and scheduling of strictly periodic tasks in multi-core real-time systems. In *Proceedings of the 22nd International Conference on Embedded and Real-time Computing Systems and Applications* (pp. 130–138). Daegu, Korea (South). [CrossRef]
- [3] Indradjad, A., Sunarmodo, W., Salyasari, N., & Pratiknyo, B. (2019). Development of national forest/land fire monitoring system using remote sensing satellite data (terra/aqua modis and snpp) by automation and nearly real-time. In *IOP Conference Series: Earth and Environmental Science* (Vol. 280, p. 012032). [CrossRef]
- [4] Cai, W., Qian, P., Ding, Y., Bi, M., Ning, X., Hong, D., & Bai, X. (2023). Graph Structured Convolution-Guided Continuous Context Threshold-Aware Networks for Hyperspectral Image Classification. *IEEE Transactions on Geoscience and Remote Sensing*. [CrossRef]
- [5] Cai, W., Gao, M., Ding, Y., Ning, X., Bai, X., & Qian, P. (2023). Stereo Attention Cross-Decoupling Fusion-Guided Federated Neural Learning for Hyperspectral Image Classification. *IEEE Transactions on Geoscience and Remote Sensing*. [CrossRef]
- [6] Yang, Y., Chen, H., Chen, S., Qiu, D., & Wang, L. (2021). Fire spot recognition and post-fire assessment based on full infrared spectroscopy. *Forestry and Ecological Sciences*, 36(2), 170–178. [CrossRef] 10.13320/j.cnki.hjfor.2021.0025
- [7] Roy, D. P., Boschetti, L., & Trigg, S. N. (2006). Remote sensing of fire severity: assessing the performance of the normalized burn ratio. *IEEE Geoscience and Remote Sensing Letters*, 3(1), 112–116. [CrossRef]
- [8] Tan, L., Zeng, Y., & Zhong, Z. (2016). An adaptability analysis of remote sensing indices in evaluating fire

- severity. *Remote Sensing for Natural Resources*, 28(2), 84–90.
- [9] Lu, Q., Wang, X., Cao, H., Li, W., & Wang, B. (2020). Remote sensing monitoring of forest fire in liangshan prefecture, sichuan province. *Surveying and Mapping of Geology and Mineral Resources*, 36(4), 9–12. [CrossRef]
- [10] Zhang, X. (2021). Research on prediction model and risk zoning of forest fires in liangshan prefecture, sichuan. *Chengdu University Of Technology*. [CrossRef]
- [11] Tang, Y., Wang, L., Zhao, J., & Wang, A. (2021). Monitoring "3-28" forest fire emergency disaster in sichuan muli based on remote sensing technology. *Land and Resources Informatization*(1), 12–18.
- [12] Shi, Y., Mu, C., Tian, Y., Huang, Y., Guo, R., & Sun, X. (2022). Classification of main crops in jinta county of gansu province based on landsat-8 data. *Geomatics & Spatial Information Technology*, 45 (2), 74–78+81.
- [13] Wu, W. (2022). Deep learning detection method of burned area based on landsat8 data. *China University of Geosciences Beijing*. [CrossRef]
- [14] Gemitzi, A., & Koutsias, N. (2022). A google earth engine code to estimate properties of vegetation phenology in fire affected areas—a case study in north evia wildfire event on august 2021. *Remote Sensing Applications: Society and Environment*, 26, 100720. [CrossRef]
- [15] Rao, Y., Wang, C., & Huang, H. (2020). Forest fire monitoring based on multisensor remote sensing techniques in muli county, sichuan province. *Journal of Remote Sensing*, 24(5), 559–570.
- [16] Ma, W. (2012). Design and implementation of pre-processing algorithm for part code recognition based on android platform. *Beijing University of Posts and Telecommunications*. [CrossRef]
- [17] Chen, Z. (2012). Remote sensing image processing based on gray morphology open operation. *Technology Innovation and Application*(10), 18.
- [18] Dwornik, M., Porzycka-Strzelczyk, S., Strzelczyk, J., Malik, H., Murdzek, R., Franczyk, A., & Bala, J. (2021). Automatic detection of subsidence troughs in sar interferograms using mathematical morphology. *Energies*, 14(22), 7785. [CrossRef]
- [19] Zhang, Q. (2007). Study on the technology of large space fire detection based on image processing. *Xihua University*.
- [20] Zhang, Y., Wang, M., & Wang, J. (2018). Risk analysis of forest fires and protection of forest resources in china based on information diffusion theory. *Environmental Protection*, 46(19), 38–43. [CrossRef]
- [21] Chen, J., Li, M., Yuan, Z., & Gu, Q. (2020). An improved a* algorithm for uav path planning problems. In *Proceedings of the 4th Information Technology, Networking, Electronic and Automation Control Conference* (Vol. 1, pp. 958–962). Chongqing, China. [CrossRef]
- [22] Nuthammachot, N., & Stratoulis, D. (2021). Multi-criteria decision analysis for forest fire risk assessment by coupling ahp and gis: Method and case study. *Environment, Development and Sustainability*, 1–16. [CrossRef]
- [23] Liu, M., Cheng, L., Gu, Y., Wang, Y., Liu, Q., & O'Connor, N. E. (2021). MPC-CSAS: Multi-party computation for real-time privacy-preserving speed advisory systems. *IEEE Transactions on Intelligent Transportation Systems*, 23(6), 5887-5893. [CrossRef]
- [24] Zhang, X., Cui, L., Shen, W., Zeng, J., Du, L., He, H., & Cheng, L. (2023). File processing security detection in multi-cloud environments: a process mining approach. *Journal of Cloud Computing*, 12(1), 100. [CrossRef]
- [25] Liu, C., Zeng, Q., Cheng, L., Duan, H., Zhou, M., & Cheng, J. (2021). Privacy-preserving behavioral correctness verification of cross-organizational workflow with task synchronization patterns. *IEEE Transactions on Automation Science and Engineering*, 18(3), 1037-1048. [CrossRef]
- [26] Li, J., Li, J., Xie, C., Liang, Y., Qu, K., Cheng, L., & Zhao, Z. (2023). PipCKG-BS: A Method to Build Cybersecurity Knowledge Graph for Blockchain Systems via the Pipeline Approach. *Journal of Circuits, Systems and Computers*, 2350274. [CrossRef]
- [27] Li, S., Li, J., Pei, J., Wu, S., Wang, S., & Cheng, L. (2023). Eco-CSAS: A Safe and Eco-Friendly Speed Advisory System for Autonomous Vehicle Platoon Using Consortium Blockchain. *IEEE Transactions on Intelligent Transportation Systems*. [CrossRef]
- [28] Chen, X., Yu, Q., Dai, S., Sun, P., Tang, H., & Cheng, L. (2023). Deep Reinforcement Learning for Efficient IoT Data Compression in Smart Railroad Management. *IEEE Internet of Things Journal*. [CrossRef]
- [29] Wang, Y., Wang, Y., Shi, C., Cheng, L., Li, H. and Li, X., (2020). An edge 3D CNN accelerator for low-power activity recognition. *IEEE Transactions on Computer-Aided Design of Integrated Circuits and Systems*, 40(5), pp.918-930. [CrossRef]
- [30] Cheng, L., Wang, Y., Liu, Q., Epema, D. H., Liu, C., Mao, Y., & Murphy, J. (2021). Network-aware locality scheduling for distributed data operators in data centers. *IEEE Transactions on Parallel and Distributed Systems*, 32(6), 1494-1510. [CrossRef]
- [31] Liu, J., Shen, H., Chi, H., Narman, H. S., Yang, Y., Cheng, L., & Chung, W. (2021). A low-cost multi-failure resilient replication scheme for high-data availability in cloud storage. *IEEE/ACM Transactions on Networking*, 29(4), 1436-1451. [CrossRef]
- [32] Chen, X., Cheng, L., Liu, C., Liu, Q., Liu, J., Mao, Y., & Murphy, J. (2020). A WOA-based optimization approach for task scheduling in cloud computing systems. *IEEE Systems Journal*, 14(3), 3117-3128. [CrossRef]



Yiwei Hua Currently studying for the fourth year in the College of Information Science and Engineering, Henan University of Technology. Spatial Information and Digital Technology.



Xingdong Wang Currently working at the School of Information Science and Engineering, Henan University of Technology. His current research interests include remote sensing, GIS (geographic information system).